

Rheological and Thermal Properties of Polylactide/Organic Montmorillonite Nanocomposites

Biao Wang, Tong Wan, Wei Zeng

College of Material Science and Chemical Engineering, Tianjin University of Science and Technology, Tianjin 300457, China

Received 23 November 2011; accepted 8 January 2012

DOI 10.1002/app.36770

Published online in Wiley Online Library (wileyonlinelibrary.com).

ABSTRACT: Polylactide/organic montmorillonite (PLA/OMMT) nanocomposites were prepared by melt-compounding technique. Dynamic and steady rheological properties, as well as dynamic mechanical and thermal stability of the nanocomposites were evaluated using various characterization tools. It was found that the rheological behaviors of nanocomposites were related with both temperatures and OMMT loadings. At low OMMT loadings, the steady-shear viscosities and the complex viscosities showed a Newtonian plateau in low frequency region or low shear rate region. At high OMMT loadings, strong shear-thinning behaviors were observed in the full range of frequencies or shear rates. The complex viscosities and the storage modulus gradually decreased in the full frequency

region with increasing temperature. The results demonstrated that rheology of PLA/OMMT nanocomposites was mainly sensitive to OMMT loadings. The relaxation time spectrum indicated that the relaxation of the PLA macromolecular chains was strongly confined by the layers of OMMT. The mechanical properties measured by dynamic mechanical analysis (DMA) and tensile test, and thermal stability of PLA/OMMT nanocomposites were improved at low OMMT loadings. © 2012 Wiley Periodicals, Inc. *J Appl Polym Sci* 000: 000–000, 2012

Key words: PLA; montmorillonite; rheology; viscoelastic properties; nanocomposites

INTRODUCTION

It is well known that majority of existing materials are derived from nonrenewable fossil resources, which will eventually be extinguished. Consequently, there is a need for the development of “green” materials that would be relied on renewable resources. They would not involve the use of toxic or noxious components in their manufacture, and could naturally take place degradation with composting or could be recycled easily. Polylactide (PLA) derived from a renewable agricultural resource (corn) is of increasing commercial interest due to easy degradation by simple hydrolysis.^{1–3}

PLA has good mechanical properties, thermal plasticity, and biocompatibility, thus being a promising polymer for various end-use applications.^{4–6} However, some drawbacks, such as brittle nature and a lack in toughness, poor thermal stability, and melt strength, are disadvantageous in practical processing

especially in the film extrusion industry. Of particular commercial interest is recently developing nanocomposite technology consisting of a polymer and organically modified layered silicate such as montmorillonite, mica, talc etc., which often exhibits remarkably improved mechanical and various other properties as compared to those of virgin polymers.^{7–10}

Rheological properties are useful in evaluating polymer resins for their suitability in processing operations¹¹ and can be used to gauge and predict the molecular orientations that are formed in these materials while in the molten stage during processing and when frozen to final products. These frozen stresses lead to anisotropy in physical quantities and affect its end use properties. The melt rheological behavior of neat PLA was widely reported earlier. High L-content polylactide exhibited strain hardening in extension and that the Cox–Merz rule is obeyed far into the shear-thinning region.¹² The melt rheology of both branched and linear grade of PLA was investigated by Dorgan et al.¹³ They concluded that longer relaxation times in the terminal region for the branched material compared to the linear material manifested itself as a higher zero shear rate viscosity and the branched material shear thins more strongly, resulting in a lower value of viscosity at high shear rates.

In the case of polymer/layered silicate nanocomposites, the measurements of rheological properties are not only important to understand the knowledge

Correspondence to: B. Wang (wb22@tust.edu.cn).

Contract grant sponsor: Scientific Research Foundation of Tianjin University of Science & Technology; contract grant number: 20090405.

Contract grant sponsors: Scientific Research Foundation for the Returned Overseas Chinese Scholars, State Education Ministry.

of the processability of these materials, but is also helpful to find out the strength of polymer-layered silicate interactions and the structure–property relationship in nanocomposites.¹⁴ In our previous studies, we have reported on the preparation, dynamic rheology, structure, and morphology of PLA/organic montmorillonite (OMMT) nanocomposites.¹⁵ In this case, the intrinsic properties of neat PLA were comparatively improved after incorporating with OMMT. The main purpose of this work is to further understand the effect of OMMT on the steady rheology, mechanical properties, and thermal stability of PLA/OMMT nanocomposites.

EXPERIMENTAL

Material and preparation of nanocomposites

Poly(lactide (PLA) polymer 4060D, a product from NatureWorks® (registered trademark of Cargill Dow, Minnetonka, Hennepin, Minnesota) was used in this study. This grade of NatureWorks® PLA is amorphous with average molecular weight of 1.4×10^5 and polydispersibility index of 1.5 as measured by gel permeation chromatography (GPC). The OMMT (NB-901) modified by octadecylammonium ions were supplied by Huate Chemical Co., Ltd, Zhejiang, China.

PLA pellets and OMMT powder were dried in a vacuum oven at 50°C for 24 h to remove moisture prior to melt compounding process. PLA with various OMMT loadings were melt compounded in a Haake PolyLab Rheomix 600 p at 180°C and 30 rpm for 6 min till the torque reached constant. Neat PLA as a reference was processed in the Haake mixer under the same conditions for comparison. The film samples were prepared from the blends of PLA and OMMT by heat pressing at 180°C. Some strands of the blends were placed in a compression mold to ensure a constant size ($90 \times 60 \times 0.7 \text{ mm}^3$) and covered with aluminum foil sheets to prevent the press plates from sticking to each other. This assembly was then placed between the press plates for 3 min without applying pressure, until the material was sufficiently melted, and then pressed for 2 min at a pressure of 10 MPa. The whole assembly with the press plates was then cool pressed for 3 min at a pressure of 10 MPa. The compression molded specimens were then stored in a desiccator awaiting analysis. The sample was designated as neat PLA, PLAM1, PLAM5, and PLAM10 according to the mass ratio of PLA/OMMT: 100/0, 99/1, 95/5, and 90/10, respectively.

Characterization

Prior to rheological measurements, the compression-molded specimens were cut into the disks with 25 mm in diameter and dried at 50°C for 24 h.

A strain-controlled rotational rheometer (Physica, MCR300, Austria) was employed to measure the viscoelastic response of PLA/OMMT nanocomposites. The measurements were carried out in dynamic (oscillatory) mode as well as steady (rotational) mode by means of 25 mm parallel geometry with a fixed gap of 0.5 mm in the temperature range from 170 to 230°C under nitrogen atmosphere. Amplitude sweeps were performed in advance to ensure that dynamic tests were in the linear viscoelastic range and the strain value of 1% was consequently chosen. Frequency range from 0.1 to 100 rad s^{-1} and shear rate range from 10^{-1} to 100 s^{-1} were applied for dynamic and steady tests, respectively.

Dynamic mechanical analysis was performed on a Netzsch DMA-242 dynamic mechanical analyzer (German). The average sample size was $25 \times 4 \times 0.7 \text{ mm}^3$ and the measurements were taken in tension mode from 0 to 150°C at a heating rate of 3 $^\circ\text{C min}^{-1}$ and frequency of 1 Hz. Then, storage modulus $\log E'$ and $\tan \delta$ were recorded as a function of temperature.

Thermogravimetric analysis (TGA) was performed under nitrogen atmosphere from 50 to 600°C at a heating rate of 10 $^\circ\text{C min}^{-1}$ by using a Perkin-Elmer TGA 7.

Dumbbell-shaped specimens were prepared at 180°C with hot-press molding. The tensile tests were carried out on an Instron 1121 machine at room temperature with a crosshead speed of 50 mm min^{-1} , and the five average values were taken as the experimental data.

RESULTS AND DISCUSSION

Rheological properties

The effect of temperature on the complex viscosity $|\eta^*|$ and the storage modulus G' for neat PLA is shown in Figure 1. It was obvious that $|\eta^*|$ of neat PLA exhibited Newtonian liquid behavior at low angular frequency region at all temperatures from 170 to 230°C. A consistent viscosity reduction of approximately 2/3 of the previous value was observed at low frequency region for an increase in temperature of 20°C as shown in Figure 1(a). Furthermore, the onset frequency of shear-thinning (ω_{onset}) gradually increased from 1.01 to 22.64 rad s^{-1} when the temperature was increased from 170 to 230°C. Figure 1(b) showed that storage modulus decreased with decreasing frequency at each temperature for neat PLA. However, it was obviously different profile for storage modulus between 170 and 230°C. It appeared that there was an inflexion in the curves above 190°C, suggesting that storage modulus was more sensitive to temperature and the degradation of PLA molecular chains may occur at higher temperature due to the inferior thermal stability of PLA matrix. Moreover, the inflexion at 230°C apparently

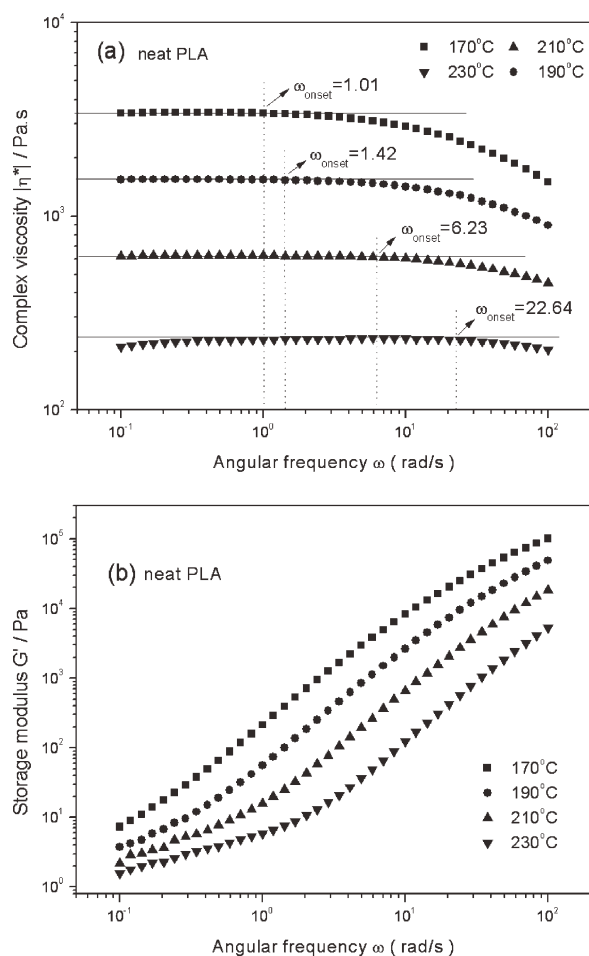


Figure 1 Effect of temperature on the complex viscosity (a) and the storage modulus (b) for neat PLA.

moved to higher frequency (shorter time) than that at 210°C, implying that the degradable process may occur more quickly at higher temperature.

The effect of temperature on the complex viscosity $|\eta^*|$ and the storage modulus G' for PLAM5 was shown in Figure 2. In contrast to neat PLA, $|\eta^*|$ of the nanocomposite with 5 wt % OMMT loading apparently showed non-Newtonian shear-thinning behavior at all temperatures as shown in Figure 2(a). Moreover, both complex viscosity and storage modulus decreased with increasing temperature. In low frequency region, PLAM5 exhibited more solid-like behavior than the neat PLA, in which the former possessed at least two order of magnitude higher G' value than the latter as shown in Figures 1(b) and 2(b). PLAM5 showed nonterminal behavior for all temperatures at the terminal zone. The nonterminal behavior was also observed for other intercalated and exfoliated polymer/clay nanocomposites.^{16–19} Such behavior could be monitored for the composites with solid fillers having a high aspect ratio at high volume fraction, or with solid fillers interacting strongly with polymer matrix.²⁰

As shown in Figure 2(b), the slope of G' in the low frequency region almost decreased to zero for PLAM5 at all temperatures. Galgali et al. has attributed the observed behavior of G' to strong solid–solid interactions in the nanocomposites.²¹ The aspect ratio of the particles in the nanocomposites reported here was very high and the percolating network was formed at a relatively low volume fraction of OMMT which was in accord with our previous rheological results.¹⁵

The dependence of the steady-shear viscosity (η) on shear rate ($\dot{\gamma}$) (solid symbols), and that of the dynamic complex viscosity ($|\eta^*|$) on angular frequency (ω) (open symbols) for neat polymer and the nanocomposites are shown in Figure 3. At low shear rates, the neat PLA and PLAM1 exhibited Newtonian liquid behavior while all of the nanocomposites exhibited non-Newtonian shear-thinning behavior. Especially, the viscosity diverged at low shear rates for two nanocomposites with the high OMMT loading. We have previously observed the presence of pseudo-solid-like behavior for these concentrations near quiescent conditions, resulting from a percolated filler network and strong filler–filler interactions.²²

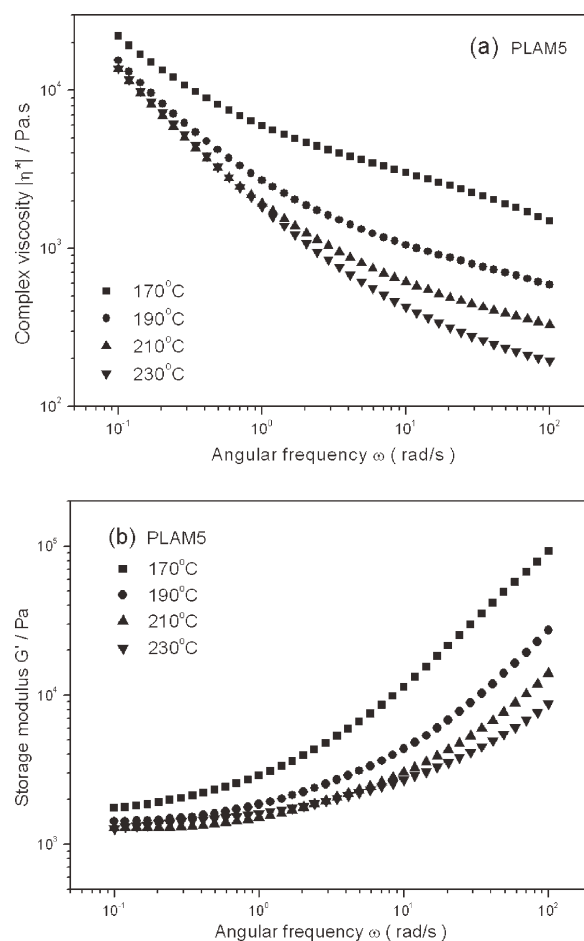


Figure 2 Effect of temperature on the complex viscosity (a) and the storage modulus (b) for PLAM5.

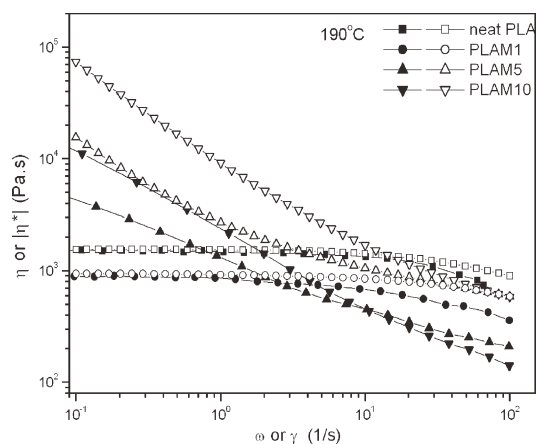


Figure 3 Comparison between complex viscosity $|\eta^*|$ (open symbol) vs. frequency ω and the steady-state shear viscosity η (solid symbol) vs. shear rate $\dot{\gamma}$ for neat PLA and PLA/OMMT nanocomposites at 190°C.

The neat PLA roughly obeys the empirical Cox–Merz rule, which requires that for $\dot{\gamma} = \omega$, the viscoelastic data should obey the relationship $\eta(\dot{\gamma}) = |\eta^*(\omega)|$. PLAM1 exhibited minor deviations from the Cox–Merz rule, with $|\eta^*|$ exceeding η outside of the errors of measurement especially at high shear rate as shown in Figure 3. Further, PLAM5 and PLAM10 did not follow the Cox–Merz rule at all shear rates, as observed for other mesostructure materials.²³ The measured $|\eta^*|$ for the two nanocomposites exceeded η at all shear rates, which was contrary to the results reported by Dealy et al.²⁴ No changes to the quiescent mesostructure were expected due to the small displacements in the linear dynamic oscillatory measurements; however, it would be expected that the mesostructure be considerably altered during the steady-shear measurements. Therefore, significant alignment of the silicate layers and tactoids might occur even at the lowest measured shear rates of steady shear.

It was suggested that the enhanced shear-thinning at low shear rates or angular frequencies observed in Figure 3 could result from the PLA, confined between particles and layers, experiencing a much larger effective strain rate due to the confinement.²⁵ This confinement was correlative with not only the OMMT loading as expected but also with the temperature as discussed later.

However, the non-Newtonian behavior and strong shear-thinning characteristic at low shear rates can be attributed to the ability of steady shear to orient the highly anisotropic layers or tactoids. Additionally, at high shear rates, the steady-shear viscosities for the nanocomposites were lower than that of neat PLA. These observations suggested that the layers were strongly oriented in the flow direction at high shear rates and silicate layers or tactoids dominated the shear viscosity and shear-thinning at high shear rates.

In Figure 4, the continuous relaxation time spectrum H as a function of relaxation time λ , which was calculated from storage modulus obtained in dynamic mode by rheological analysis software, was

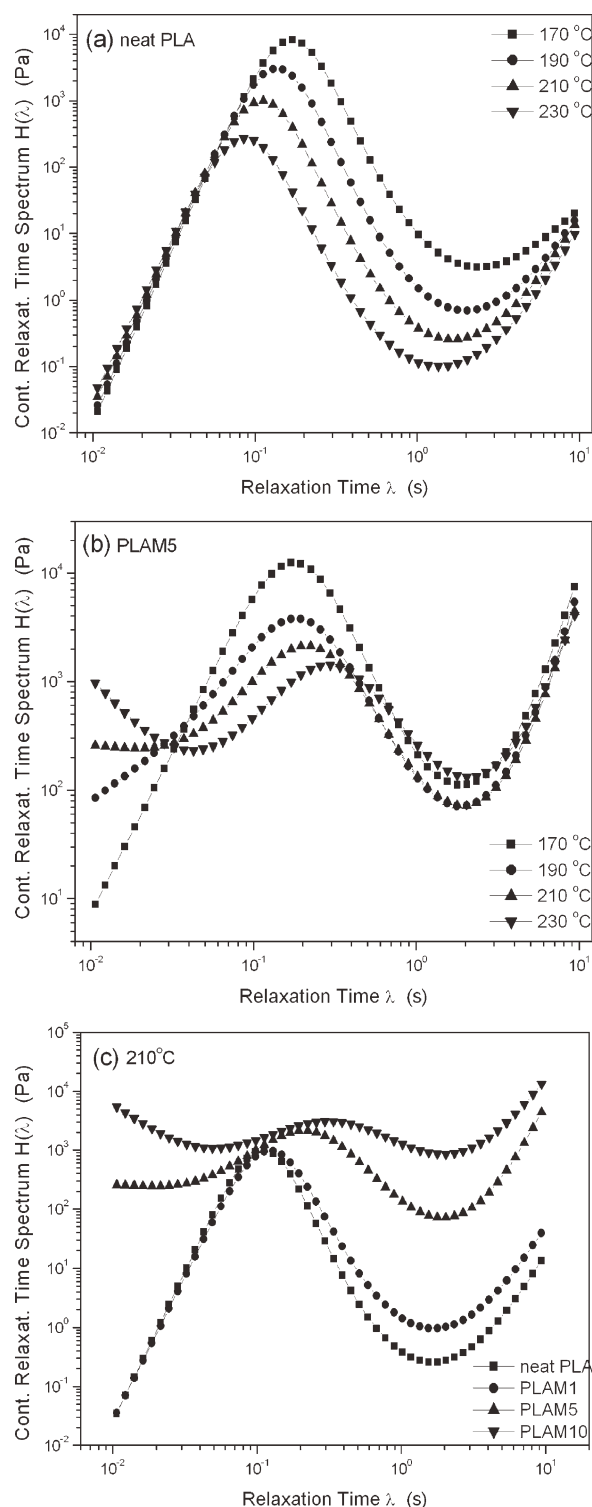


Figure 4 Relaxation time λ dependence of the continuous relaxation time spectrum H at four temperatures for neat PLA (a) and PLAM5 (b). Effect of OMMT loadings on the continuous relaxation time spectrum H at 210°C (c).

TABLE I
The Values of λ_{\max} and H_{\max} for neat PLA and PLAM5

Sample	T ($^{\circ}\text{C}$)	λ_{\max} (s)	H_{\max} (Pa)
Neat PLA	170	0.17	8280
	190	0.13	3030
	210	0.11	997
	230	0.08	270
PLAM5	170	0.17	12,500
	190	0.20	3780
	210	0.22	2120
	230	0.30	1410

shown in logarithmic coordinate for neat PLA and nanocomposites. Their maxima represent concentrations of relaxation processes in certain regions of the logarithmic time scale. At long relaxation times, when steady flow is reached, H becomes very small on the logarithmic scale in uncrosslinked viscoelastic melts. For viscoelastic solid, H attains quite low values at long time but gives no evidence of approaching zero. This behavior is associated with the persistence of a small negative slope in stress relaxation, showing that some degree of relaxation continues to longer times. At very short time, if the mechanical behavior approaches perfect elasticity, H remains finite, and in these polymers at a rather high level, some relaxation processes occur even at the shortest times, because of dissipative processes at the highest frequencies.²⁶

As expected, both the maximum value of H (H_{\max}) and the value of λ_{\max} (λ at H_{\max}) for neat PLA gradually decreased with increasing temperature from 170 to 230 $^{\circ}\text{C}$ as shown in Figure 4(a) and Table I. For example, the values of λ_{\max} reduced from 0.17 to 0.08 s and that of H_{\max} decreased from 8280 to 270 Pa when the temperature increased from 170 to 230 $^{\circ}\text{C}$. It suggested that the relaxation process of molecular chains occurred more quickly at higher temperature for neat PLA. On the contrary, for the PLA/OMMT nanocomposites, the dependence of chains relaxation process on the temperature was apparently different from the neat PLA. Figure 4(b) showed continuous relaxation time spectrum H versus relaxation time λ at different temperatures for PLAM5. In contrast with neat PLA, the values of λ_{\max} increased with increasing temperature and the values of λ_{\max} and H_{\max} were also listed in Table I. This meant that the chains relaxation process of PLA/OMMT nanocomposites was slowed with increasing temperature, suggesting enhanced confinement effect for PLA chains among silicate layers at higher temperature.

In addition, the effect of OMMT loadings on continuous relaxation time spectrum was also shown in Figure 4(c). It was expected that the value of λ_{\max} shifted toward longer time with increasing OMMT loadings, implying that the higher the OMMT load-

ing, the greater the relaxation time. In other words, the confinement effect in the nanocomposites with high OMMT loadings was stronger than that in nanocomposites with low ones.

Thermal stability

The thermal stability of neat PLA and the nanocomposites also has been investigated by TGA under nitrogen flow as shown in Figure 5. The charring residues were about 7.84, 4.54, 0.84, and 0.01 wt % for PLAM10, PLAM5, PLAM1, and neat PLA, respectively, as shown in Figure 5(a). Figure 5(b) was the enlarged photograph of selected region in Figure 5(a). The onset of decomposition temperature (at weight loss of 5 wt %) was slightly improved by about 3 $^{\circ}\text{C}$ at low nanofiller loadings (less than 5 wt %). In contrast, at high OMMT loadings (such as 10 wt %) the nanocomposite degraded at temperature 3 $^{\circ}\text{C}$ inferior to the degradation of the neat PLA matrix as shown in Figure 5(b). However, all the TGA traces showed a shift of the weight loss toward higher temperature, for example, with stabilization as high as about 2 $^{\circ}\text{C}$ at 50 wt % weight loss for PLAM10 nanocomposite. It was usually accepted that the improved thermal stability for polymer/clay nanocomposites is mainly due to the formation of char, which hinders the out-diffusion of the volatile decomposition products, as a direct result of the decrease in permeability, usually observed in exfoliated nanocomposites.²⁷

However, for the studied PLA/OMMT system, it seemed that the enhanced thermal stability was only achieved at low OMMT loading level and the improvement in thermal stability was much more significant for exfoliated nanocomposites than that for the intercalated ones. Optimal thermal stabilization was achieved at OMMT concentration below 5 wt %, as also observed in ethylene vinyl acetate copolymer (EVA)/clay²⁷ and nylon 11/clay nanocomposites.¹⁰ Despite this, the exact degradation mechanism was currently not clear; this behavior was probably associated with the morphological changes in relative proportion of exfoliated and intercalated species with the OMMT loadings. At low OMMT loadings (e.g., 1 wt %), exfoliation dominated but the amount of exfoliated silicate layers was not enough to enhance the thermal stability through char formation.²⁴ With increasing OMMT loadings (e.g. 5 wt %), much more exfoliated silicate layers were formed, char forms more easily and effectively and consequently promotes the thermal stability of the nanocomposites. At even higher OMMT loading level (e.g. 10 wt %), the intercalated structure was the dominant population and even if char was formed in high quantity, the morphology of the nanocomposites probably did not allow for

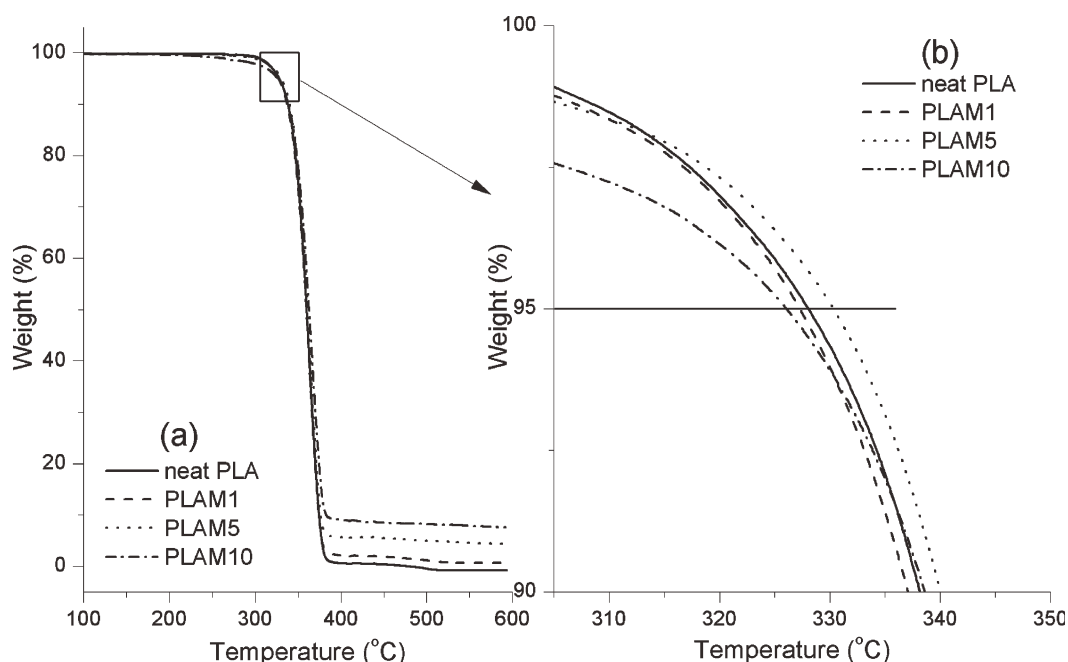


Figure 5 (a) Temperature dependence of weight loss for PLA/OMMT nanocomposites in nitrogen flow. (b) Enlarged image of selected region in (a).

maintaining a good thermal stability. However, it was known that the chemical nature of the studied polymers and the type of clay or montmorillonite used played an important role in their degradation behavior. Thus, care should be taken when explaining this behavior in PLA in comparison with other polymer system, as observed in poly(etherimide)/clay nanocomposites where intercalated nanolayers were found to have better thermal stability than the exfoliated ones.²⁸

Dynamic mechanical analysis

Figure 6(a) shows the spectra of dynamic storage modulus E' versus temperature T for neat PLA and PLA/OMMT nanocomposites. Usually, E' can describe the stiffness of material. The addition of OMMT increased the E' of PLA/OMMT nanocomposites within tested temperature range. The E' of PLA improved from 4.71 to 7.41 GPa on the addition of 10 wt % OMMT at 40°C within glassy plateau and it increased by about 25% at 100°C within rubbery plateau from 20.21 (neat PLA) to 25.36 MPa (PLAM10). The significant improvement in the E' of PLA/OMMT nanocomposites was ascribed to the effect of good dispersion and high performance of OMMT filler. Sternstein and Zhu studied the reinforcement mechanism of nanofilled polymer at a temperature higher than T_g and suggested that the principle mechanism for reinforcement is confined entanglements.²⁹ The adhesion interaction between polymer chains and filler surfaces led to confined entanglements, which had both near and far field

effect on matrix chain motion and played the role of physical crosslinking in the system, thus causing greatly enhanced modulus of the matrix.³⁰ Therefore, a nanofilled polymer with higher modulus can be manufactured. The role of physical crosslinking in the semicrystalline polymer appeared to be less important than crystalline one. On the other hand, when the load was transferred to the physical crosslinking network, the confined effect from the filler surface may impede the relaxation of the matrix entanglement structure, thus leading to lower toughness. Furthermore, it was obvious that the value E' of PLAM5 was higher than that of PLAM1 and PLAM10. When the content of OMMT exceeded 5 wt %, the value E' of nanocomposite decreased and it may be attributed to readily aggregation and stronger interaction between OMMT layers at high OMMT loading due to high aspect ratio and large surface area. This confirmed the so called "percolation threshold" again which was consistent with our previous results of melt-rheology measurements.¹⁵

The viscoelasticity is the typical characteristic of all polymer materials. The strain lags the cyclical sinusoidal stress exerted in the DMA experiment. Damping factor $\tan \delta$ is expressed as follow: $\tan \delta = E''/E'$, where E'' is the loss modulus and E' is the storage modulus. The temperature dependence of $\tan \delta$ for neat PLA and PLA/OMMT nanocomposites is shown in Figure 6(b). Generally speaking, the location and intensity of the $\tan \delta$ can be used to evaluate the toughness of polymer materials. The higher the intensity and the lower the peak

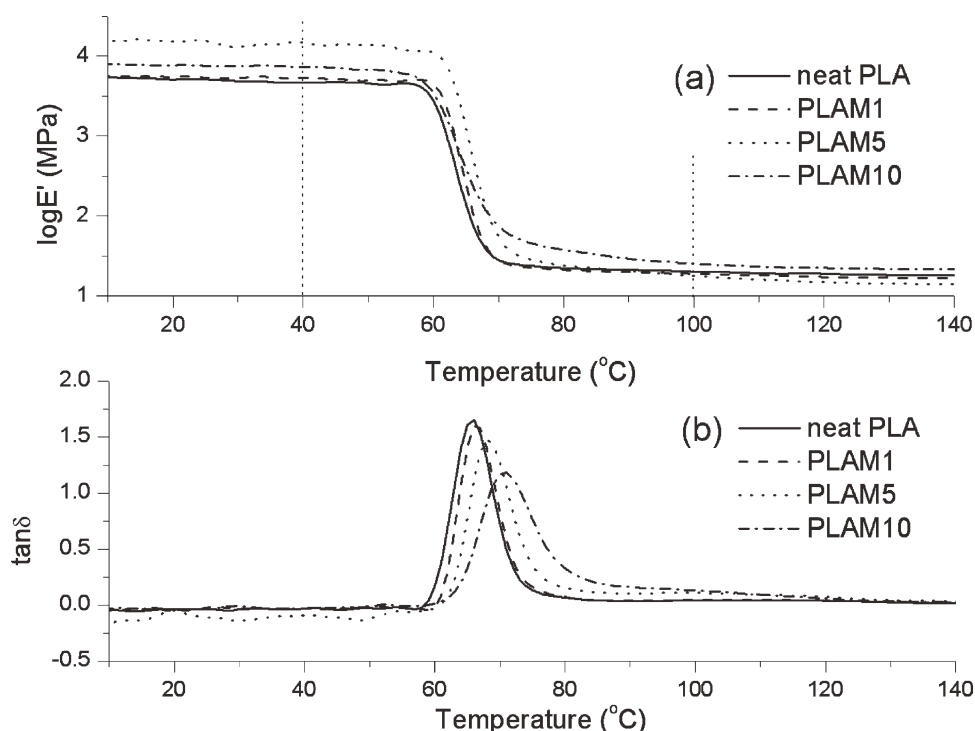


Figure 6 Dynamic mechanical properties of PLA and PLA/OMMT nanocomposites as a function of temperature, (a) storage modulus $\log E'$ (b) damping factor $\tan \delta$.

temperature of the $\tan \delta$ results in, the better the toughness of the polymer materials hold. From Figure 6(b) it was observed that the temperature of $\tan \delta$ peak of neat PLA was at 65.7°C and the value of $\tan \delta$ was 1.65; they were 66.4°C and 1.60 in PLAM1; 68.4°C and 1.48 in PLAM5; 70.7°C and 1.18 in PLAM10, respectively. These results indicated that the addition of OMMT into PLA deteriorated slightly the toughness of the matrix in accordance with the previous analysis. In the meantime, the stiffness of the matrix increased due to the presence of OMMT. The incorporation of OMMT into PLA matrix obvi-

ously increased the glass transition temperature (T_g), probably implying that more constraint from two-dimensional layered nanofiller was imposed on polymer molecular chains. It was different from the case of reinforced-polymer materials by the one-dimensional nanofiller such as carbon nanotube, in which the mobility of polymer molecular chains was less confined by the carbon nanotube bundles, thus almost unvarying the T_g of the nanocomposites.³¹

Mechanical properties analysis

Typical stress-strain curves of the neat PLA, PLAM1, and PLAM5 are shown in Figure 7. The corresponding result of sample PLAM10 was not shown due to the much brittle nature and difficult specimen preparation. A noticeable yield and post yield drop was observed for neat PLA and PLA/OMMT nanocomposites. It can be seen that addition of OMMT significantly improved the tensile properties of PLA matrix, as summarized in Table II. Upon incorporation of only 1 wt % OMMT, the tensile

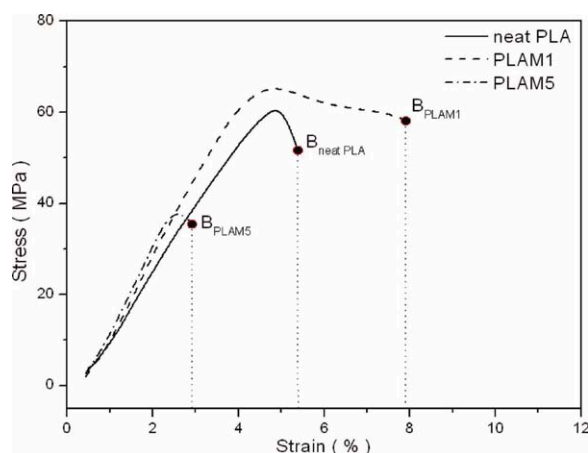


Figure 7 Stress-strain curves for neat PLA and PLA/OMMT nanocomposites. [Color figure can be viewed in the online issue, which is available at wileyonlinelibrary.com.]

TABLE II
Tensile Properties of Neat PLA and PLA/OMMT Nanocomposites

Sample	σ (MPa)	E (MPa)	ϵ (%)
Neat PLA	61.9	1654.8	5.4
PLAM1	65.2	1927.1	7.9
PLAM5	39.1	1945.2	2.9

strength at yield was improved by about 5.3% from 61.9 to 65.2 MPa, and the tensile modulus of PLA was improved by about 16.5% from 1654.8 to 1927.1 MPa. The increased elongation at break (7.9%) for PLAM1 indicated that PLAM1 became more ductile compared with neat PLA which broke at elongation of 5.4%.

However, the addition of more OMMT loading (5 wt %) into PLA matrix significantly decreased the tensile strength at yield stress (from 61.9 to 39.1 MPa) and elongation at break (from 5.4 to 2.9%) except for tensile modulus (from 1654.8 to 1945.2 MPa). In many cases,²⁵ the increase in the tensile modulus of polymers by compounding with silicate, like clay, sacrificed the elongation at break. However, the tensile modulus and elongation at break of PLAM1 as shown in Table II and Figure 7 were all superior to that of neat PLA. Thus, the prominent mechanical properties of exfoliated nanocomposites were obviously observed in this work.

CONCLUSIONS

The rheological behaviors of PLA/OMMT nanocomposites showed a dependence on both temperature and OMMT loadings. For neat PLA and the nanocomposite with low OMMT loadings (1 wt %), the complex viscosities showed a Newtonian plateau in low frequency region at low temperature. The nanocomposites with high OMMT loadings exhibited a strong shear-thinning behavior. The dependence of relaxation behaviors on temperature for nanocomposites was different from that for neat PLA, which was attributed to the confinement effect of two-dimensional anisotropic layered silicate. TGA showed that thermal stability of the nanocomposites was slightly improved by about 3°C when the OMMT loading is up to 5 wt %. However, the stabilization significantly decreased at higher OMMT loading probably owing to the transformation in morphology of the nanocomposites and relatively poor OMMT dispersion. DMA showed that the addition of OMMT enhanced the stiffness and significantly diminished the toughness of PLA matrix. The mechanical properties were significantly improved for the exfoliated PLA/OMMT nanocomposites with low OMMT loadings.

References

- Höglund, A.; Hakkarainen, M.; Albertsson, A. C. *Biomacromolecules* 2010, 11, 277.
- Nieddu, E.; Mazzucco, L.; Gentile, P.; Benko, T.; Balbo, V.; Mandrile, R.; Ciardelli, G. *React Funct Polym* 2009, 69, 371.
- Carfi Pavia, F.; La Carrubba, V.; Brucato, V. *Int J Mater Forming* 2009, 2, 713.
- Yuryev, Y.; Wood-Adams, P. *J Polym Sci Part B: Polym Phys* 2010, 48, 812.
- Drumright, R. E.; Gruber, P. R.; Henton, D. E. *Adv Mater* 2000, 12, 1841.
- Lunt, J. *Polym Degrad Stab* 1998, 59, 145.
- Nam, J. Y.; Ray, S. S.; Okamoto, M. *Macromolecules* 2003, 36, 7126.
- Chen, G. X.; Kim, H. S.; Shim, J. H.; Yoon, J. S. *Macromolecules* 2005, 38, 3738.
- Giannelis, E. P.; Krishnamoorti, R.; Manias, E. *Adv Polym Sci* 1999, 138, 107.
- Liu, T. X.; Lim, K. P.; Tjiu, W. C.; Pramoda, K. P.; Chen, Z. K. *Polymer* 2003, 44, 3529.
- Ramkumar, D. H. S.; Bhattacharya, M. *Polym Eng Sci* 1998, 38, 1426.
- Palade, L. I.; Lehermeier, H. J.; Dorgan, J. R. *Macromolecules* 2001, 34, 1384.
- Dorgan, J. R.; Lehermeier, H. J.; Mang, M. *J Polym Environ* 2000, 8, 1.
- Ray, S. S.; Okamoto, M. *Macromol Mater Eng* 2003, 288, 936.
- Wang, B.; Wan, T.; Zeng, W. *J Appl Polym Sci* 2011, 121, 1032.
- Feng, W.; Kadi, A.; Riedl, B. *Macromol Rapid Commun* 2002, 23, 703.
- Solomon, M. J.; Almusallam, A. S.; Seefeldt, K. F.; Somwamgthanaroj, A.; Varadan, P. *Macromolecules* 2001, 34, 1864.
- Hyun, Y. H.; Lim, S. T.; Choi, H. J.; Jhon, M. S. *Macromolecules* 2001, 34, 8084.
- Krishnamoorti, R.; Giannelis E. P. *Macromolecules* 1997, 30, 4097.
- Han, C. D. *Multiphase Flow in Polymer Processing*; Academic Press: New York, 1981.
- Galgali, G.; Ramesh, C.; Lele, A. *Macromolecules* 2001, 34, 852.
- Park, C.; Kim, M. H.; Park, O. O. *Polymer* 2004, 45, 1267.
- Larson, R. G. *The Structure and Rheology of Complex Fluids*; Oxford University Press: New York, 1999.
- Dealy, J. M.; Wissbrun, K. F. *Melt Rheology and Its Role in Plastic Processing*; Van Nostrand Reinhold: New York, 1990.
- Subbotin, A.; Semenov, A.; Manias, E.; Hadziioannou, G.; Ten Brinke, G. *Macromolecules* 1995, 28, 1511.
- Ferry, J. D. *Viscoelastic Properties of Polymers*; Wiley: New York, 1980.
- Alexandre, M.; Dubois, P. *Mater Sci Eng* 2000, 28, 1.
- Lee, J.; Takekoshi, T.; Giannelis, E. P. *Mater Res Soc Symp Proc* 1997, 457, 513.
- Sternstein, S.; Zhu, A. J. *Macromolecules* 2002, 35, 7262.
- Vacatello, M. *Macromolecules* 2002, 35, 8191.
- Wang, B.; Sun, G. P.; He, X. F.; Liu, J. *J Polym Eng Sci* 2007, 47, 1610.